Astronomy & Astrophysics manuscript no. d+20
June 26, 2020

Dispersion Measure variability for 36 millisecond pulsars at low frequencies

J. Y. Donner[1,2], J. P. W. Verbiest[2,1], W. A. Coles[3], C. Tiburzi[4], S. Osłowski[5], J. Künsemöller[2], A.-S. Bak Nielsen[1,2], N. Porayko[1], M. A. Krishnakumar[2], J.-M. Grießmeier[6,7], M. Serylak[8,9], M. Kramer[1,10], J. M. Anderson[11,12], O. Wucknitz[1], and PWG

[1] Max-Planck-Institut für Radioastronomie, Auf dem Hügel 69, 53121 Bonn, Germany
[2] Fakultät für Physik, Universität Bielefeld, Postfach 100131, 33501 Bielefeld, Germany
[3] ECE Dept., University of California at San Diego, La Jolla, CA, 92093-0407, U.S.A
[4] ASTRON, the Netherlands Institute for Radio Astronomy, Oude Hoogeveensedijk 4, 7991 PD Dwingeloo, The Netherlands
[5] Centre for Astrophysics and Supercomputing, Swinburne University of Technology, PO Box 218, Hawthorn, Victoria 3122, Australia
[6] LPC2E – Université d'Orléans / CNRS, 45071 Orléans cedex 2, France
[7] Station de Radioastronomie de Nançay, Observatoire de Paris, PSL Research University, CNRS, Université d'Orléans, OSUC, 18330 Nançay, France
[8] SKA South Africa, The Park, Park Road, Pinelands 7405, South Africa
[9] Department of Physics and Astronomy, University of the Western Cape, Private Bag X17, Bellville 7535, South Africa
[10] Jodrell Bank Centre for Astrophysics, University of Manchester, M13 9PL, UK
[11] Technical University of Berlin, Institute of Geodesy and Geoinformation Science, aculty VI sec. H 12, Straße des 17. Juni 135, 10623 Berlin, Germany
[12] GFZ German Research Centre for Geosciences, Telegrafenberg, 14473 Potsdam, Germany

Received date / Accepted date

ABSTRACT

Context. Radio pulses from pulsars are affected by a frequency-dependent propagation delay due to interstellar dispersion. Variations in the magnitude of this effect lead to an additional source of red noise in pulsar-timing experiments.
Aims. We aim to quantify the time-variable dispersion with much-improved precision and characterise the spectrum of these variations.
Methods. We use the pulsar-timing technique to get highly precise dispersion measure (DM) time series of single-observation measurements. Our dataset consists of 36 sources that were observed for up to 7.1 years with the LOw Frequency ARray (LOFAR) telescope at a centre frequency of ~ 150 MHz. 17 of these sources were observed on weekly cadence.
Results. We achieve a median DM precision of a few 10^{-5} cm^{-3}pc for a significant fraction of our sample. We detect significant variations of the DM in all pulsars with a median DM uncertainty of less than $2 \cdot 10^{-4}$ cm^{-3}pc. The observed variations add extra noise in pulsar timing experiments at a level of 100 ns to 10 μs at 1.4 GHz over a timespan of a few years. We did not detect a frequency dependence of the DM for any of the sources in our dataset.
Conclusions. The DM time series we obtained from LOFAR observations could in principle be used to correct higher-frequency data for the variations of the dispersive delay. However, there is currently the practical restriction that pulsars tend to provide either highly precise times of arrival (ToAs) at 1.4 GHz or a high DM precision at low frequencies, but not both.

Key words. pulsars: general – ISM: structure – gravitational waves

1. Introduction

Pulsars are highly magnetised, rapidly rotating neutron stars, the remnants of massive stars that ended their lives in a supernova explosion. At their magnetic poles, pulsars emit beams of electromagnetic radiation, which is most pronounced at radio frequencies. As the neutron star rotates, these beams sweep around in space due to the fact that the magnetic and spin axes are generally not aligned. If any of the beams cross the line of sight to the Earth, we detect regular pulses of radiation at our telescopes. While the shape of individual pulses can vary significantly, the average pulse shape when integrating over hundreds of pulses is usually very constant, which allows for an accurate measurement of the times of arrival (ToAs) of the pulses. General information on pulsars was described and summarised by Lorimer & Kramer (2005).

There are two major distinct populations of pulsars: the normal, slow pulsars with pulse periods of the order of ∼1 s and the millisecond pulsars (MSPs). The latter are thought to be spun up at some point in their evolutionary history, which is why they are also called 'recycled' pulsars. MSPs are of particular scientific interest as the much shorter pulse periods allow for a more precise determination of the ToAs and their rotation was found to be much more stable (Hobbs et al. 2010; Verbiest et al. 2009).

Pulsar timing The high rotational stability of pulsars, and MSPs in particular, allows for precise modelling of the pulsar's astrophysical properties with a so-called "timing model", a method

called pulsar timing (see Lorimer & Kramer 2005). The model is usually improved by inspecting the timing residuals (i.e. the difference between the measured ToAs of the pulses and the ones predicted by the model).

Pulsar Timing Arrays One major application of pulsars are the so-called pulsar timing array (PTA) projects, which aim to detect low-frequency gravitational waves (see, e.g. Hobbs & Dai 2017; Tiburzi 2018; Burke-Spolaor et al. 2019). The basic idea behind these experiments is that passing gravitational waves would distort the spacetime in a way that the arrival times of some pulsars will be delayed while the pulses of other pulsars arrive earlier at the telescope. By observing a large number of precisely-timed pulsars over a long time span, a gravitational wave would be measurable in the correlation of the timing residuals of different pulsars. To achieve a high precision in these experiments, many sources of noise have to be taken into account, one of which is the interstellar medium (ISM).

Influence of the interstellar medium The ISM contains ionised particles. An electromagnetic wave passing through the medium will experience a frequency-dependent change in group velocity, a phenomenon called *dispersion*. Specifically, this implies an additional delay Δt in the ToAs, which can be approximated as (see Lorimer & Kramer 2005):

$$\Delta t = D\frac{\mathrm{DM}}{\nu^2}, \tag{1}$$

where $D \simeq 4.149 \times 10^3\,\mathrm{MHz^2\,pc^{-1}\,cm^3\,s}$ is the dispersion constant[1], ν the observing frequency (expressed in MHz) and DM is the "dispersion measure" (expressed in $\mathrm{cm^{-3}pc}$), which is defined as:

$$\mathrm{DM} = \int_0^d n_\mathrm{e}(l)\mathrm{d}l, \tag{2}$$

where d is the distance to the pulsar (expressed in pc) and n_e is the electron density (in $\mathrm{cm^{-3}}$).

As the pulsar moves, our line of sight passes through different parts of the ionised ISM (IISM), which implies a temporal variability in the DM due to inhomogeneities in the IISM. The variations in the DM lead to a significantly variable dispersive delay (see Eq. 1) and thus add a source of noise to the timing.

Using relatively high observing frequencies minimises the impact of DM variations on the ToAs as the dispersive delay scales with ν^{-2} (see Eq. 1). However, the IISM turbulence spectrum is steep with significantly more power at larger scales (Armstrong et al. 1995), so for long timing campaigns, the dispersive delays will sooner or later still have a significant impact on the ToAs. Also, the observing frequency cannot be increased indefinitely, as pulsars have rather steep spectra (Bates et al. 2013), which leads to a loss of S/N at very high frequencies. Lazarus et al. (2016) detected MSPs at 5 GHz and even 9 GHz, some of which had a sub-1 μs precision at 5 GHz, so this approach can work for some flat-spectrum sources.

A more gernerally applicable solution is to correct for the time-variable dispersive delays by subtracting them from the ToAs, which effectively gives the ToA at infinite frequency. One approach to achieve this is to use multi-frequency observations or split wide-band observations into multiple subbands, but these kinds of observations are not always available in PTA experiments (see, e.g. Desvignes et al. 2016). A problem of this approach follows from Equation 12 of Lee et al. (2014): the correction for the DM increases the uncertainty of the infinite-frequency ToA. This effect is especially large at high frequencies and small fractional bandwidths, so correcting typical PTA ToAs at 1.4 GHz with DMs measured from the same observation would greatly increase the ToA uncertainty (by about an order of magnitude for a 250-MHz wide frequency band).

Another approach is to use low-frequency observations to measure the DM very precisely and use these measurements to correct the higher-frequency ToAs, which are more sensitive to the pulsar and less affected by IISM effects. One potential complication of this approach is the possibility of frequency-dependent DMs (Cordes et al. 2016; Donner et al. 2019), which are caused by the fact that due to interstellar scattering, the ray paths through the medium are frequency dependent.

This paper In this paper, we present precise DM time series of 36 MSPs using low-frequency (~150 MHz) observations with a particular focus on pulsars used in PTA experiments. In Section 2 we describe our observational setup and our sources, while Section 3 explains our data analysis. We discuss our findings in Section 4 and conclude our results in Section 5.

2. Observations

The observations used in this paper were taken with the International LOw Frequency ARray (LOFAR) Telescope (ILT) which is described in detail by van Haarlem et al. (2013).

Specifically, we used the data of two different pulsar monitoring campaigns. One uses the LOFAR core stations situated in the North-East of the Netherlands to observe the sources of interest with monthly cadence for up to 7.1 years between 2012-12-19 and 2020-01-14. The pulsar pipeline used by the LOFAR core is described by Stappers et al. (2011). It produces data cubes with resolution in frequency (195.3125 MHz-wide channels), time (10-sec sub-integrations), polarisation (four coherency products) and rotational phase (256 to 1024 phase bins). The data were stored in TIMER format, which is similar to the PSRFITS format described in Hotan et al. (2004). Each observation has a centre frequency of 148.9 MHz, a bandwidth of 78.1 MHz (400 frequency channels) and lasts 5 to 30 minutes, depending on the pulsar brightness.

For the other campaign, the six LOFAR stations of the German LOng Wavelength (GLOW) consortium, located in Effelsberg (telescope identifier DE601), Unterweilenbach (DE602), Tautenburg (DE603), Potsdam-Bornim (DE604), Jülich (DE605) and Norderstedt (DE609), were disconnected from the ILT network and used as individual stand-alone telescopes instead. The beamformed data from the stations were sent to the Max-Planck Institut für Radioastronomie (MPIfR) and the Forschungszentrum Jülich on dedicated high-speed links, where recording computers ran the dedicated LOFAR und MPIfR Pulsare (LuMP)[2] data-taking software, which formats and otherwise prepares the beamformed pulsar data for subsequent (off-line but near-real-time) phase-resolved averaging (commonly referred to as "folding") using the DSPSR software package (van Straten & Bailes 2011). This produces data cubes in the same format as the LOFAR core pulsar pipeline. The data for this campaign

[1] Often the inverse is defined in the literature.

[2] Publicly available at `https://github.com/AHorneffer/lump-lofar-und-mpifr-pulsare` and described on `https://deki.mpifr-bonn.mpg.de/Cooperations/LOFAR/Software/LuMP`.

were taken between 2013-08-20 and 2020-01-08. The resulting dataset of these observations covers a time span of up to 6.4 years per pulsar, with a weekly cadence and typical integration times of 1 to 3 hours. The faintest pulsars which are only observed with the core are not detectable with the international stations. Early observations and the observations of DE601 have a total bandwidth of 95.3 MHz (488 frequency channels), centred at 149.9 MHz. For technical reasons, the bandwidth of the other stations was reduced to 71.5 MHz (366 channels) in February 2015. In order to minimise the impact of the bandwidth reduction on the scientific quality of our data, the centre frequency was shifted to align the observed bandwidth with the most sensitive part of the bandpass, resulting in a new centre frequency of 153.8 MHz. This implies a shift in centre frequency by an integer number of frequency channels (20), so that the frequencies of individual channels remained constant over the entire dataset.

Table 1 shows detailed information on the observation characteristics for each source. We excluded PSR J1939+2134 (PSR B1937+21) from our analysis because its strongly variable scattering has a significant impact on the DM estimation. Also, due to the very strong scattering, the scattering tail of the pulse profile merges with the next pulse, so the profile is very wide. Observations at higher frequencies or more advanced analysis techniques could lead to more robust and similarly precise DM measurements.

3. Data Analysis

The main measure of interest in this paper are DM time series. In the following, we will describe what kind of processing we applied to the "raw" data, how we calculated the ToAs and how we measured the DM.

3.1. Pre-processing

The basic processing in this work has been carried out with the PSRCHIVE (Hotan et al. 2004; van Straten et al. 2012) software package. As a first step, the data were cleaned from radio frequency interference (RFI), by using a modified version of the "Surgical" algorithm of the CLEAN.PY script from the COASTGUARD (Lazarus et al. 2016) python package.[3] In the rare case of outliers due to remaining RFI, the observations were also manually inspected and additional cleaning was applied using the PSRCHIVE program PAZI. On average, 9.1% of data were removed in this process.

The data were calibrated in polarisation following the methods outlined in Noutsos et al. (2015) using the DREAMBEAM[4] python package to calculate the Jones matrices. For some pulsars (especially PSR J2145−0750) this significantly improved the reduced χ^2 values of the DM fits.

To make the dataset as homogeneous as possible, the bandwidth of all observations has been reduced to 70.3 MHz (i.e. 360 channels, centred at 153.2 MHz). To achieve this, 2 empty dummy channels had to be added at the top of the band for the LOFAR core observations.

[3] The version we used was provided by Künkel (2017) and is publicly available at `https://github.com/larskuenkel/iterative_cleaner`.

[4] Publicly available at `https://github.com/2baOrNot2ba/dreamBeam`, by T. Carozzi.

3.2. Timing

For the International Pulsar Timing Array (IPTA) pulsars, we took the timing model from the first IPTA data release (Verbiest et al. 2016, data combination B)[5], and removed any existing DM models (including Solar wind) or FD parameters[6], as we are interested in the time evolution of the DM and the FD parameters were derived at higher frequencies. To account for the different time span over which the IPTA ephemerides were derived, and because the DM estimates are expected to be more precise at the low radio frequencies of LOFAR, we performed an initial timing analysis over our dataset, with the aim of updating the reference DM for each pulsar. For this initial timing analysis, we derived an analytic template from a single, bright observation by fitting a few von-Mises functions (see, e.g., Jammalamadaka & SenGupta 2001) to the total intensity profile of the observation using the program PAAS. The functions are implemented in the form:

$$f(x) = A \cdot e^{\kappa \cdot (\cos(2\pi(x-\mu))-1)} \tag{3}$$

with A being the amplitude of the component, κ the compactness and μ pulse phase. x is defined such that one full rotation corresponds to $x = 1$. To obtain the ToAs, we used the FDM[7] algorithm of the program PAT on copies of our observations with reduced frequency resolution (integrated down to 10 frequency channels). We then used the TEMPO2 software (Hobbs et al. 2006) to fit for DM and applied the result to our data archives. This prevents smearing of the pulse profile when partly integrating the data in frequency.

For the non-IPTA pulsars, we took our initial timing model from the ATNF Pulsar Catalogue (PSRCAT)[8] by Manchester et al. (2005). For PSR J1658+3630, there was no timing model available in the catalogue, so we used the timing model from Sanidas et al. (2019). We then did a similar analysis, but also fit for parameters describing the pulsar's rotation and, if needed, the position of the pulsar and its orbit in binary systems.

For some pulsars in our sample (e.g. PSR J0740+6620), there is still significant structure in the timing residuals, due to timing noise, strong DM variations, the Solar wind or a combination of these. To proceed with the analysis described as follows, we created additional timing models containing many rotational frequency and DM derivatives as well as a simple, spherically-symmetric Solar-wind model to align the observations.

Once optimised the timing model, we created a data-derived standard template for each pulsar by averaging the observations from the observing site that monitored that pulsar the most. As the S/N of most observations is rather low (rarely above 100), we integrated the template in frequency to between six and 30 channels, depending on the pulsar brightness. We then applied wavelet smoothing to the template with the program PSRSMOOTH (Demorest et al. 2013), to avoid self-standarding (see Appendix of Hotan et al. 2005). With this template, we again used the FDM algorithm to calculate the ToAs, matching each frequency channel of the observation (that was frequency-integrated accordingly) with the corresponding channel of the template. With this method, any constant frequency dependence of the pulse profile

[5] Publicly available at `http://www.ipta4gw.org/`

[6] FD parameters describe a frequency-dependent, non-dispersive delay in the timing residuals, see Arzoumanian et al. (2015).

[7] This algorithm is identical to that described by Taylor (1992), except for the uncertainties. FDM uses either formal uncertainties or Monte-Carlo simulations. We used the uncertainties determined from Monte-Carlo simulations.

[8] `http://www.atnf.csiro.au/people/pulsar/psrcat/`

Table 1. Summary of observations. Given are the pulsar name in J2000 coordinates, the pulse period P, the catalogue DM, the ecliptic latitude β, the total time span of the observations, the number of observations with GLOW and the LOFAR core $n_{\rm glow}$ and $n_{\rm core}$, the value of the structure function $D_{\rm DM}$ at a time lag of 1000 days, the median DM uncertainty of individual DM measurements, the median reduced χ^2 of the individual DM fits, and the number of frequency channels in each observation. The last column shows whether the pulsar is used in different PTA projects (i.e. the European Pulsar Timing Array (EPTA), Parkes Pulsar Timing Array (PPTA) or North American Nanohertz Observatory for Gravitational Waves (NANOGrav), see Verbiest et al. 2016; Arzoumanian et al. 2018).

source name (J2000)	P (ms)	DM $\left(\frac{\rm pc}{\rm cm^3}\right)$	β (deg)	span (yrs)	$n_{\rm glow}$	$n_{\rm core}$	$D_{\rm DM}(1000\,{\rm d})$ $\left(\frac{\rm pc^2}{\rm cm^6}\right)$	med($\sigma_{\rm DM}$) $\left(10^{-5}\,\frac{\rm pc}{\rm cm^3}\right)$	med$\left(\frac{\chi^2}{n_{\rm free}}\right)$	$n_{\rm chan}$	PTA
J0030+0451	4.9	4.3	1.4	7.0	355	79	2.28e-08	16	1.0	10	E N
J0034−0534	1.9	13.8	−8.5	7.0	1041	78	1.63e-08	3	1.0	20	E
J0218+4232	2.3	61.2	27.0	6.5	539	74	6.24e-06	35	0.9	10	E
J0407+1607	25.7	35.6	−4.7	6.4	386	65	5.02e-07	56	1.0	10	-
J0621+1002	28.9	36.5	−13.3	7.0	10	74	2.14e-04	568	1.3	10*	E
J0645+5158	8.9	18.2	28.9	6.9	268	4	1.86e-08	7	0.9	10	N
J0740+6620	2.9	15.0	44.1	4.8	261	0	8.32e-07	4	1.0	10*	N
J0751+1807	3.5	30.2	−2.8	7.1	0	71	2.05e-06	89	0.6	10*	E
J0952−0607	1.4	22.4	−17.9	2.9	37	33	3.80e-08	14	1.0	8*	-
J1012+5307	5.3	9.0	38.8	7.1	1210	79	8.62e-08	12	1.2	10	E N
J1022+1001	16.5	10.3	−0.1	7.1	1224	80	2.53e-09	12	1.2	20	E P N
J1024−0719	5.2	6.5	−16.0	7.1	5	81	8.99e-07	80	0.9	8*	E P N
J1125+7819	4.2	11.2	62.5	4.8	282	0	3.01e-07	8	0.8	10	N
J1300+1240[a]	6.2	10.2	17.6	7.1	377	80	7.63e-07	9	0.7	30	-
J1400−1431	3.1	4.9	−2.2	4.3	145	49	4.78e-07	6	0.8	8*	-
J1544+4937	2.2	23.2	65.9	5.6	5	53	5.53e-08	59	1.0	6*	-
J1552+5437	2.4	22.9	70.7	3.7	0	41	5.03e-07	7	0.9	10*	-
J1640+2224	3.2	18.4	44.1	7.1	435	79	3.84e-08	18	0.8	8	E N
J1658+3630	33.0	3.0	58.7	2.6	164	6	4.83e-07	18	0.9	10	-
J1713+0747	4.6	16.0	30.7	7.0	7	79	5.75e-08	29	0.6	10*	E P N
J1730−2304	8.1	9.6	0.2	6.5	0	74	1.92e-06	49	0.8	10*	E P
J1738+0333	5.9	33.8	26.9	7.1	0	77	4.22e-06	110	0.7	6*	E N
J1744−1134	4.1	3.1	11.8	7.0	372	79	4.84e-08	19	0.9	10	E P N
J1853+1303	4.1	30.6	35.7	6.5	1	72	3.34e-07	50	0.8	8*	E N
J1857+0943[b]	5.4	13.3	32.3	7.1	0	75	1.45e-06	82	1.3	10*	E P N
J1911−1114	3.6	31.0	11.1	7.0	0	74	2.57e-06	68	0.9	10	E
J1918−0642	7.6	26.6	15.4	7.0	0	75	2.58e-06	136	0.8	10*	E N
J1923+2515	3.8	18.9	46.7	6.6	0	73	3.30e-07	15	0.9	10*	N
J1944+0907	5.2	24.4	29.9	6.5	35	64	5.53e-06	80	0.8	6*	N
J1955+2908[c]	6.1	104.5	48.7	6.6	0	74	2.38e-05	273	0.9	10*	E N
J2043+1711	2.4	20.7	34.0	6.7	3	71	1.18e-07	18	0.9	10*	N
J2051−0827	4.5	20.7	8.8	6.5	6	74	3.07e-06	29	0.7	10*	-
J2145−0750	16.1	9.0	5.3	7.0	1010	81	6.59e-08	9	1.1	20	E P N
J2222−0137	32.8	3.3	8.0	3.8	129	41	7.79e-08	48	0.9	10*	-
J2302+4442	5.2	13.7	45.7	6.2	0	71	6.23e-06	51	0.8	10*	N
J2317+1439	3.4	21.9	17.7	7.0	381	77	1.34e-06	6	0.8	10*	E N

* For these pulsars, an analytic standard template without frequency resolution was used.
[a] PSR B1257+12
[b] PSR B1855+09
[c] PSR B1953+29

is modelled by the template and will not affect our measurement of DM.

If the templates generated in the above procedure were too noisy (due to a low S/N in the observations and a low number of observations), the smoothing produced unphysical features in the profile shape. In these cases we used an analytic template without frequency resolution, created in the same way as in the initial analysis. In principle, this would imply the need of FD parameters in the timing model to account for the frequency-dependent profile shape, but in practice the frequency dependence is not significant, as it is proven by the median χ^2 of the DM fits being close to unity (see Table 1).

3.3. Calculation of the DM

To get a precise time series of the DM, we used TEMPO2 to fit for DM for each observation individually. This approach avoids any correlation of the measured DMs with other (time-dependent) timing parameters. To handle outlier ToAs, we repeatedly applied the following rules until no ToA was removed in the iteration:

- Calculate the timing residuals r_i for the given observation using the TEMPO2 GENERAL2 plugin.
- $k = \text{mean}\left(\frac{|r_i|}{\sigma_i}\right)$. Set $k = 1$ if $k < 1$.
- If $\frac{|r_i|}{\sigma_i} > 4k$, reject the corresponding ToA.
- Fit for DM with TEMPO2.

The iterative process is necessary because there can be a significant slope in the initial residuals because of the DM variations. This is also why the factor k was introduced, as without it, ToAs at the edges of the band would be removed in the presence of a dispersive slope. This procedure is similar to that in Tiburzi et al. (2019). We expect less than ten ToAs across our entire dataset to fulfill the rejection condition simply as a consequence of random noise, so the vast majority of rejected ToAs are indeed outliers for physical reasons. The outliers were caused by a low S/N in the corresponding frequency channel, which can occur due to the pulsar being intrinsically faint at that frequency, short integration times, removal of large parts of that frequency range due to RFI, remaining low-level RFI or a combination of these. On average, 0.8% of the ToAs of an observation were removed during this step, mostly at the edges of the band were the telescope is less sensitive. While the median reduced χ^2 of the final DM fits is close to unity for all pulsars in our sample (see Table 1) and the distribution is strongly peaked around 1, there are observations not following this distribution with reduced $\chi^2 \gg 1$. These cases occur when most ToAs of an observation are flawed, usually because the pulsar is too faint or the entire observation is dominated by RFI. We excluded all DM measurements with a reduced $\chi^2 > 5$ from our subsequent analysis (on average 4% of all observations). Finally, we applied the standard TEMPO2 behaviour of multiplying the DM uncertainty by the square root of the reduced χ^2. To be conservative in our uncertainties and due to the low number of ToAs per fit, we only applied this behaviour for fits with reduced $\chi^2 > 1$.

The resulting DM time series are shown in figures 1 to 3. The median DM precision for each source is shown in Table 1. As the median reduced χ^2 is close to unity for all pulsars in our sample, the data are well fit by the model. From that we can rule out any significant frequency-dependent structure in the residuals or a frequency dependence of the DM as discussed in Donner et al. (2019), where we presented a system with more extreme DM variations.

To illustrate low-level variations, we also computed a running average of the DM time series. For each MJD sample, a weighted average over all observations is formed, weighting each DM value by the inverse of its variance. Additionally, the weights are reduced exponentially with time, scaled to $1/e$ of their original value over half the averaging window. We chose an averaging window of 30 days for pulsars with sharp features in their DM signal (i.e. PSRs J0030+0451, J0034−0534, J1022+1001, J1400−1431, J2145−0750 and J2317+1439) and 60 days for the rest.

4. Discussion

Most of the pulsars in our sample show DM variability on various timescales. The amplitude of these variations ranges from a few 10^{-4} cm^{-3}pc to a few 10^{-3} cm^{-3}pc over several years or less. Pulsars that don't show DM variations (e.g. PSR J1853+1303) are very faint at LOFAR frequencies, with a single-observation DM uncertainty of 2×10^{-4} or worse, so the non-detection of variations may be caused by a lack of sensitivity, and variations of the order of a few 10^{-4} cm^{-3}pc cannot be ruled out.

4.1. Solar wind

11 pulsars in our sample show the impact of the Solar wind, namely PSRs J0030+0451, J0034−0534, J0407+1607, J0645+5158, J1012+5307, J1022+1001, J1400−1438, J1730−2304, J1744−1134, J2145−0750 and J2317+1439 (see Fig. 1). The ecliptic latitude of these sources ranges from 0.1° (PSR J1022+1001) to 38.8° (PSR J1012+5307). We note that for PSR J1730−2304, there are only few observations close to the Sun due to the low cadence with the LOFAR core and thus those observations clearly stand out from the rest of the DM measurements. For some pulsars with low (<10°) absolute ecliptic latitude we do not clearly see the impact of the Solar wind due to a lack of measurement precision: PSRs J0751+1807, J2051−0827 and J2222−0137.

As shown in Tiburzi et al. (2019), the widely-used Solar-wind models are insufficient to correctly account for the highly variable Solar wind, which leads to short-term variations in the residual DMs of the order of a few 10^{-4} cm^{-3}pc, even at larger separations from the Sun (up to ∼ 50°). From our study we can confirm that a spherical model with constant amplitude (as is usually applied) does not suffice in most cases. This becomes clear in Figure 1, where the amplitude of the Solar wind strongly varies from year to year, which is expected due to the variable Solar activity.

4.2. Structure functions

To characterise the IISM turbulence that causes the DM variability, we calculate the structure function $D_{\rm DM}$ of the DM time series (see, e.g., You et al. 2007):

$$D_{\rm DM}(\tau) = \left\langle [\mathrm{DM}(t+\tau) - \mathrm{DM}(t)]^2 \right\rangle, \quad (4)$$

where the angle brackets indicate the ensamble average. As the IISM turbulence often follows a Kolmogorov spectrum (Armstrong et al. 1995), the structure function of the DM variations is expected to be a power law of the form:

$$D_{\rm DM}(\tau) \propto \tau^{5/3}. \quad (5)$$

In our analysis, we binned the structure function on a logarithmic scale. Figures 5 and 6 show the structure functions for the DM time series presented in figures 2 and 3, that is, all pulsars that are not significantly affected by the Solar wind. To confirm that our structure functions are compatible with the prediction arising from the assumption of a Kolmogorov spectrum, we simulated 100 DM time series per pulsar with the same sampling as our observations assuming a Kolmogorov power spectrum and calculated the structure functions. From this set of simulated structure functions we took the median value at each time lag as well as the 68% confidence interval.

To get an amplitude for the model, we first run a least-squares routine to fit the amplitude of a Kolmogorov power law to the modelled structure function, weighting each sample by its inverse variance. Then we fit a Kolmogorov power law plus a constant (to account for the white noise) to the observed structure function, adding the relative uncertainties of the data and the model in quadrature to obtain a relative uncertainty to use in the fit. This choice of weights in the fit accounts for the high red-noise uncertainty at large lags. Using the quotient of the two fit amplitudes, we rescaled the model to match the observed structure function.

Then we subtracted the white-noise level from the observed structure function, such that the resulting structure function only contains the effects of turbulent processes.

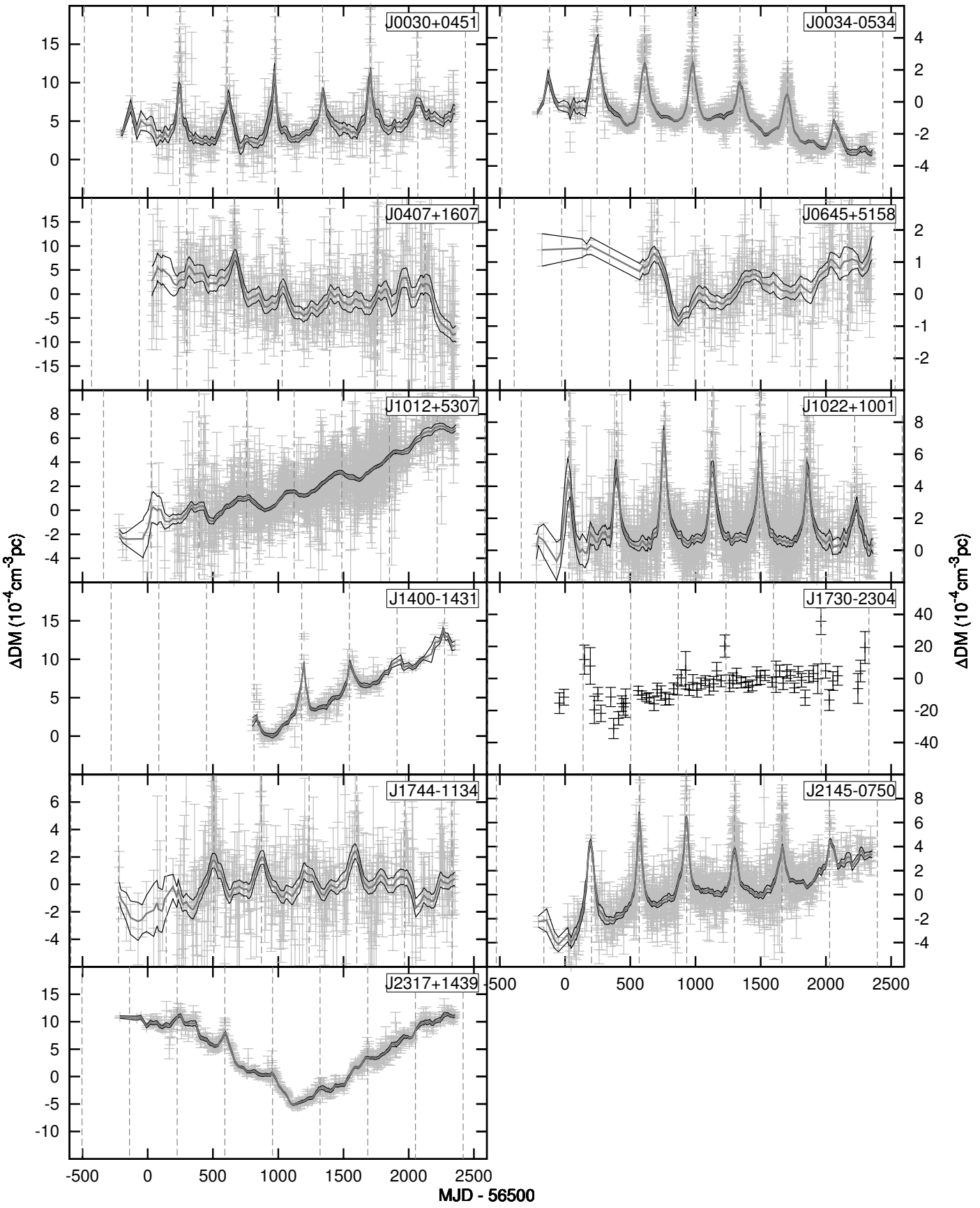

Fig. 1. DM time series for 11 MSPs that show a detectable Solar-wind signal. Individual DM measurements are plotted in grey, while running averages and their uncertainty are represented by black lines. For faint pulsars only observed with the LOFAR core, the running average is not plotted. For a clearer view, only those points with uncertainties less than 3 times the median uncertainty are plotted. The vertical lines indicate the solar approaches.

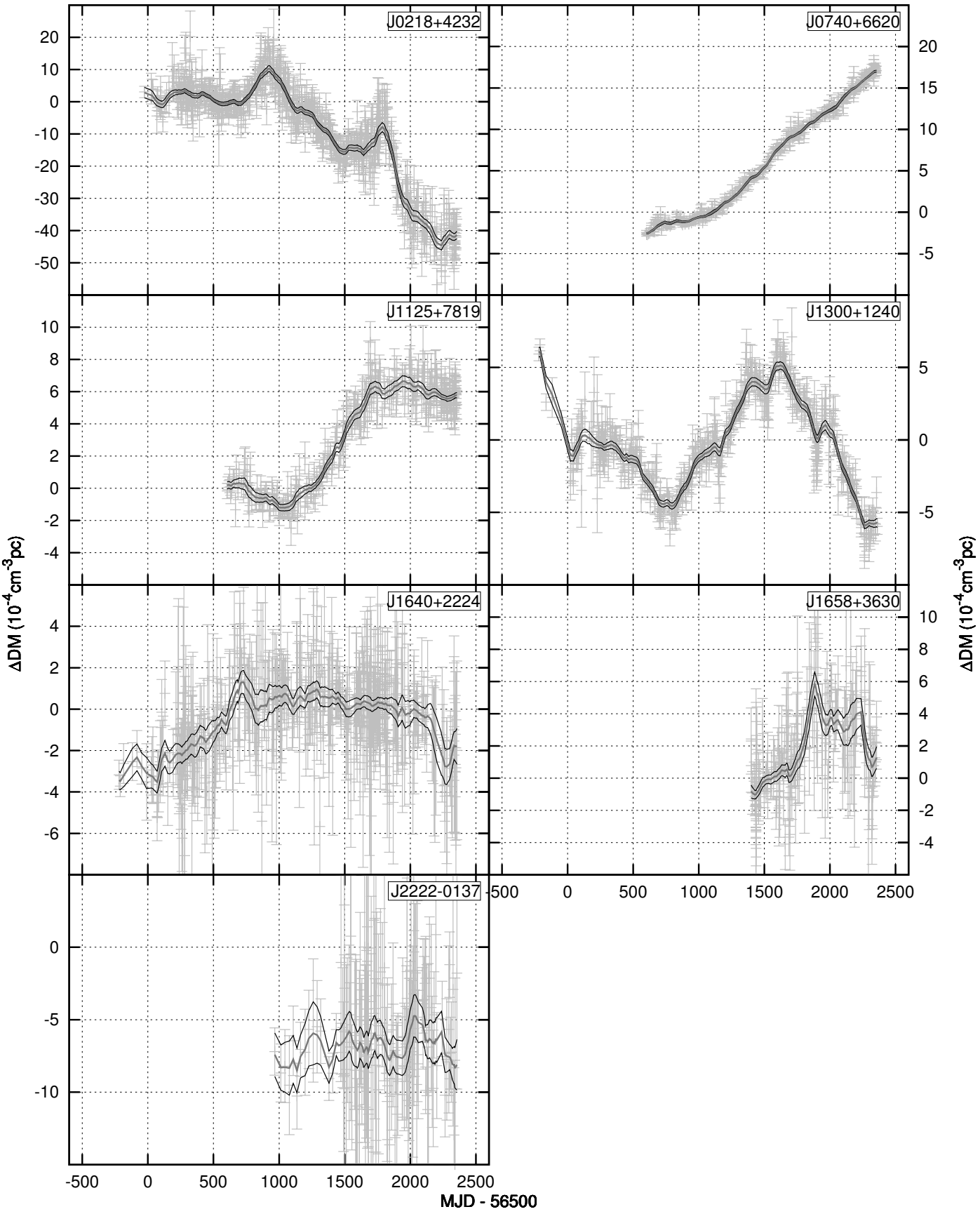

Fig. 2. DM time series for seven MSPs that were regularly observed with GLOW and do not show a clear Solar-wind signal. Otherwise same as Figure 1.

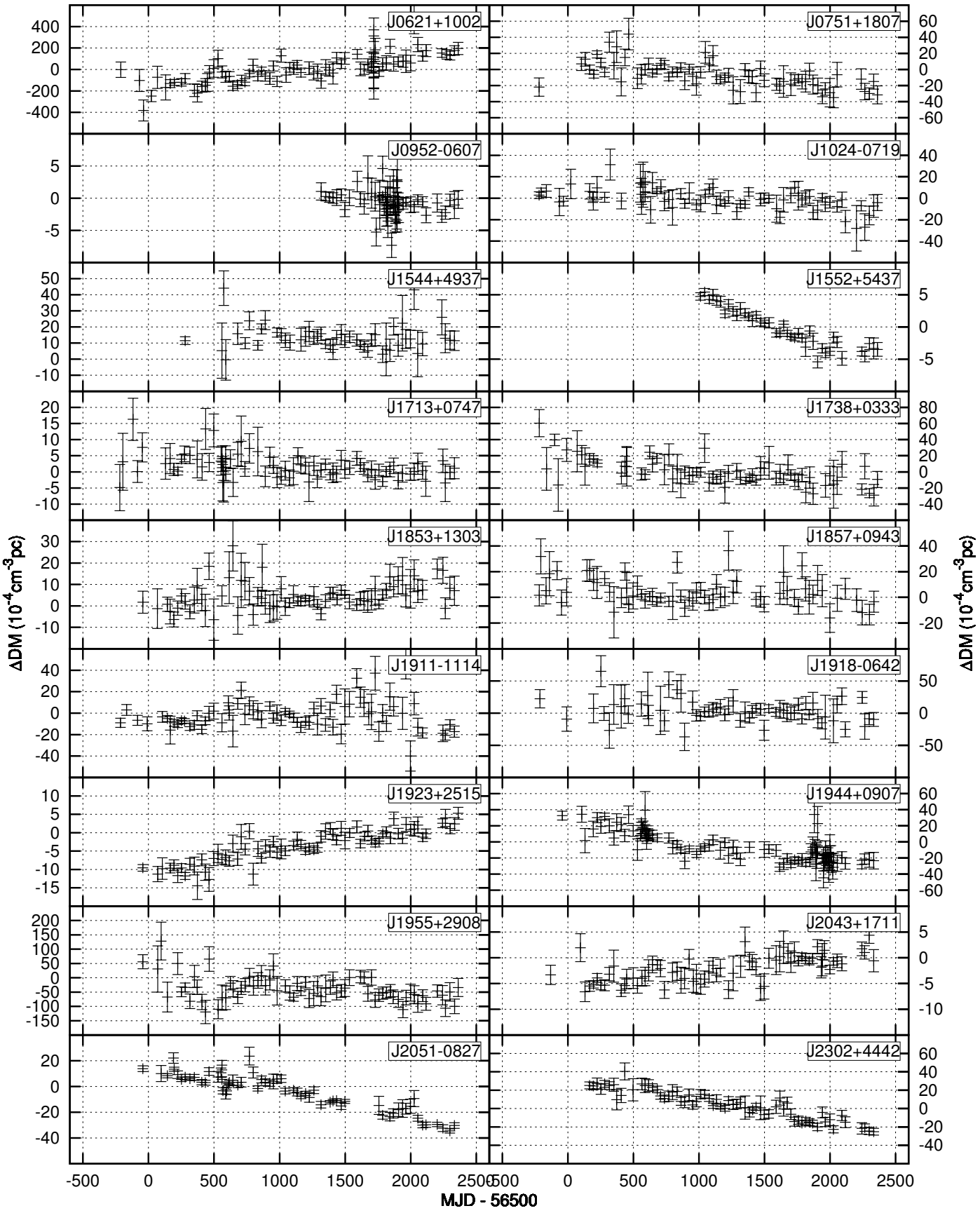

Fig. 3. DM time series for 18 faint MSPs that are only monitored regularly with the LOFAR core and do not show a clear Solar-wind signal. Otherwise same as Figure 1.

In Figure 4, we present structure functions of the DM time series which are affected by the Solar wind (Fig. 1). As we aim to quantify the IISM turbulence, we mitigated the effect of the Solar wind by sampling the DM time series when the pulsar was furthest from the Sun. We then interpolated between those samples using a cubic spline. The structure function is only calculated for time lags greater than half a year as the short-term variations are underestimated from the interpolation.

From our simulations we conclude that all our structure functions are consistent with a Kolmogorov turbulence spectrum. In the case of PSR J2222−0137, the drop in the structure function at long time lags can be explained by the fact that for the first half of our dataset, the pulsar is only observed with the LOFAR core. Those observations have a higher DM precision and therefore for the longer lags, there are only pairs containing at least one LOFAR core observation, which have a lower white noise level. From a simulation including simulations of the white noise in the DM time series, we could confirm that the drop in the structure function at long time lags is a systematic effect from our dataset.

The amplitude of the Kolmogorov structure function fit is given in Table 1.

4.3. Comparison to PTA results

DM time series of MSPs, and especially PTA pulsars, have previously been published by the various PTAs. In contrast to this study, the PTAs used higher-frequency data from their long-term timing campaigns, which usually have a lower cadence than the GLOW observations. The publications we refer to present datasets that end around the start of our dataset, making a direct comparison of the DM time series difficult.

Keith et al. (2013) use observations from three frequency bands centered at ∼700 MHz, ∼1400 MHz and ∼3100 MHz. From these data, they derive one DM estimate every three months for the 20 pulsars in their sample. As the PPTA uses the Parkes telescope (which is located in the southern hemisphere), there are only seven pulsars from their study that we also observed – all of which are at a low declination where LOFAR is not very sensitive. Keith et al. (2013) do not see clear deviations from the simple symmetric Solar-wind model they applied, but this is expected as their DM precision is not high enough. However, for some pulsars (e.g. PSR J1857+0943), their DM precision is comparable to the one achieved with LOFAR. Keith et al. (2013) also give the value of the structure function at a time lag of 1000 days, which is consistent with our results within the red-noise uncertainty.

Desvignes et al. (2016) present timing results for 42 MSPs observed with telescopes of the EPTA. The observations were taken across a range of frequencies between 350 MHz and 2.6 GHz, with the majority being taken around 1.4 GHz. From their sample, we observed 20 pulsars in this study. In their paper, they do not present DM time series, but instead use the TEMPONEST software to model the DM variations as a second-order polynomial plus a spectral noise model. This makes a comparison of individual measurements difficult, but the larger-scale trends can be compared. Whether or not the LOFAR data provide more information on the DM variability is again strongly pulsar dependent. For example, we detect a very clear DM signal in PSR J2317+1439 (see Fig. 1) while Desvignes et al. (2016) only find a DM trend at the 1σ-level, consistent with the overall trend we see in the early part of our dataset.

Jones et al. (2017) present data form the NANOGrav collaboration, analysing the DM time evolution of 37 MSPs at frequencies between 300 MHz and 2.4 GHz, 18 of which we analysed in this study. Again, the question which instrument provides a higher DM precision is pulsar dependent: LOFAR provides a much higher precision for PSR J1012+5307, whereas the higher-frequency NANOGrav data provide a much higher precision for PSR J1857+0943 (called PSR B1855+09 in Jones et al. 2017).

Overall, no inconsistency between our results and any of the mentioned PTA publications could be found. However, this is partly caused by the fact that the datasets are difficult to compare due to a lack of overlap and differences in data representation.

4.4. Consequences for PTAs

In pulsar-timing experiments, the actual ToA is often not the measure of interest. Instead, the DM-corrected, infinit-frequency ToA is the relevant measure when trying to measure IISM-independent effects. As variations in the DM at a relevant magnitude are very common, they usually have to be accounted for. In the following, we will discuss different approaches to apply corrections of the dispersive delays to ToAs at 1.4 GHz, with a timing precision of $\sigma_{\mathrm{ToA}} = 1\,\mu$s.

There are two basic approaches to consider. Approach I would be to calculate the in-band DM (as in this paper) and apply the according dispersive delay (using Eq. 1) to the timing ToAs. The uncertainty on the infinite-frequency ToA would then be

$$\sigma_\infty = \sqrt{\sigma^2_{\mathrm{ToA}} + \sigma^2_{\mathrm{disp}}}. \tag{6}$$

To avoid the dispersive correction of being the dominant factor in this example ($\sigma_{\mathrm{ToA}} = 1\,\mu$s at 1.4 GHz), the uncertainty on the DM would have to be lower than $5 \cdot 10^{-4}\,\mathrm{cm^{-3}pc}$, which would not be achievable from in-band measurements at 1.4 GHz, but potentially from simultaneous lower-frequency DM measurements as presented in this paper. Additionally, high-cadence DM time series could be smoothed to increase the precision of the dispersive corrections if the DM variations are smooth.

Approach II would be to use ToAs from multiple frequency bands and fit for the DM and T_∞ simultaneously. This has the advantage of using the entire available bandwidth, but the disadvantage that exactly-simultaneous observations may not be available, in which case short-term variability in any timing parameter has to be ruled out.

Lee et al. (2014) investigated how the choice of the observing frequencies ν_i and the corresponding ToA uncertainties σ_i affect the precision of the infinit-frequency ToAs. Equation 12 of their paper shows this relation in the case of only two observing frequencies:

$$\left\langle \delta T^2_\infty \right\rangle = \frac{\sigma_1^2\nu_1^4 + \sigma_2^2\nu_2^4}{(\nu_1^2 - \nu_2^2)^2}. \tag{7}$$

σ_∞ can be computed as the square root of the above expression. While the special case of only two ToAs is simplified, the general conclusions also hold for cases with more frequencies involved. Most importantly, the frequency band with the largest $Q = \sigma^2\nu^4$ dominates the uncertainty in T_∞. Due to the strong frequency dependence of Q, the highest frequency has to be the most-precisely measured in order to benefit from the additional bandwidth. If ν_1 is our most precise timing frequency and observations at ν_2 are used to calculate T_∞ ($\sigma_2 > \sigma_1$), Figure 7 illustrates that ν_2 should be smaller than ν_1 to achieve a timing precision close to σ_1. If ν_2 is the larger frequency, σ_∞ is limited

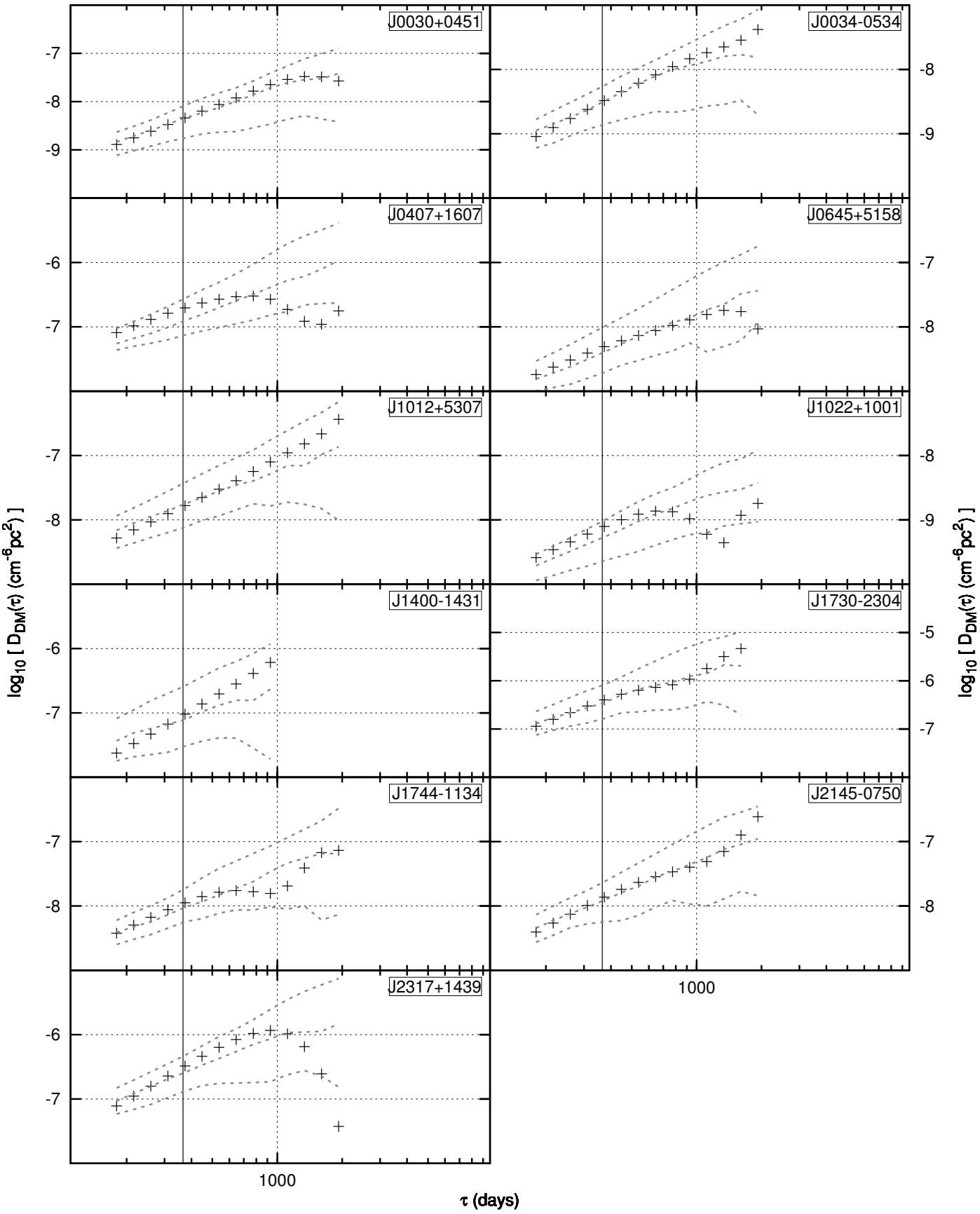

Fig. 4. Structure functions for the DM time series presented in Figure 1 after mitigation of the Solar-wind signal. The dashed lines indicate the median and 68% confidence interval of the Kolmogorov structure function simulations (see text for details). The vertical line is plotted at $\tau = 1$ yr.

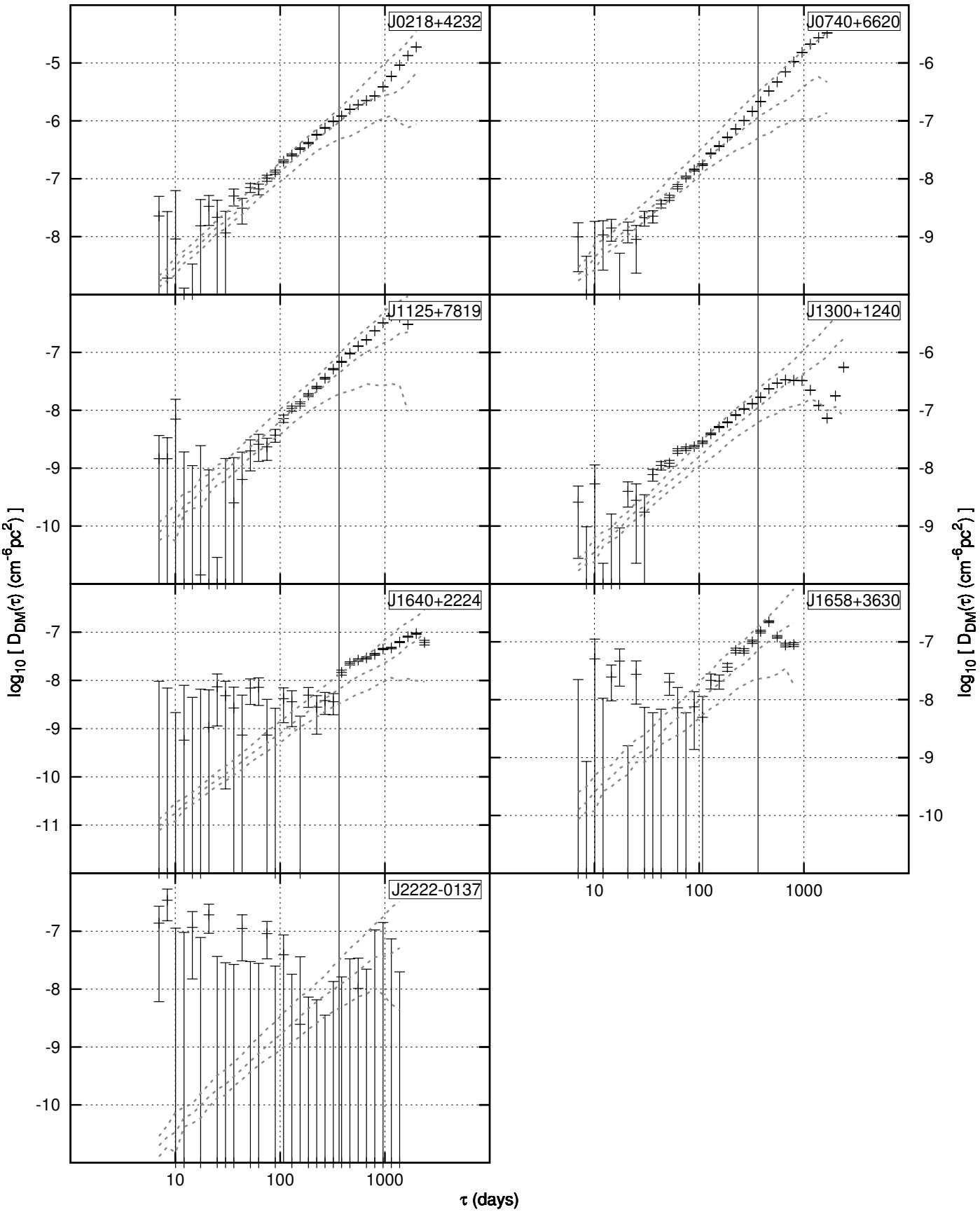

Fig. 5. Structure functions for the DM time series presented in Figure 2. The white noise level has been subtracted from the data and the Kolmogorov model. Otherwise same as Figure 4.

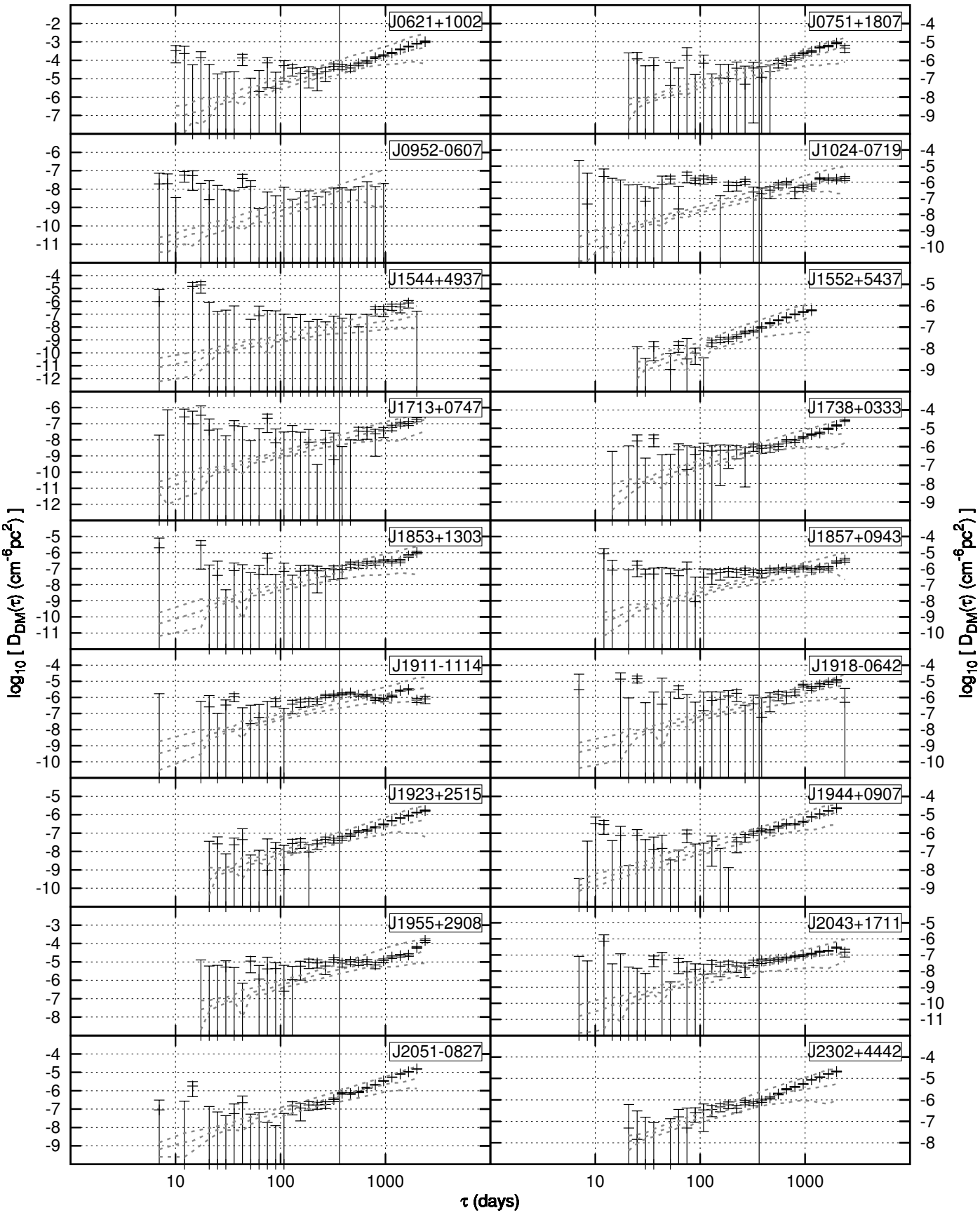

Fig. 6. Same as Figure 5, but for the DM time series presented in Figure 3.

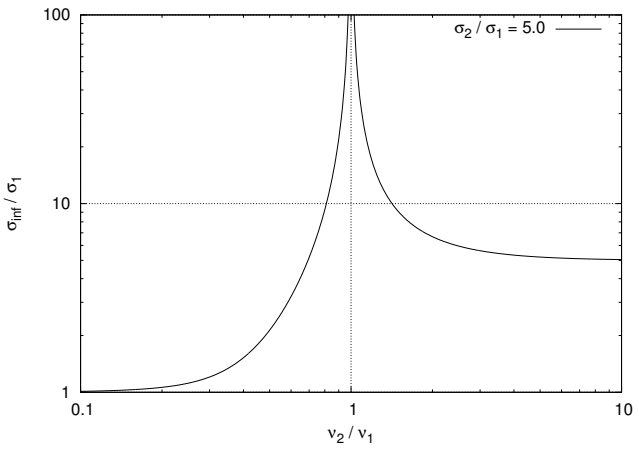

Fig. 7. Illustration of Equation 7 (Eq. 12 in Lee et al. 2014) for an observation at two frequency bands. The uncertainty of the infinite-frequency ToA is plotted as a function of ν_2, with band 2 providing less precise ToAs than band 1 ($\sigma_2 = 5.0\sigma_1$). All quantities are given relative to the frequency and ToA uncertainty of band 1. On the left side of the plot ($\nu_2 \ll \nu_1$), σ_∞ approaches σ_1, whereas on the right side ($\nu_2 \gg \nu_1$) it approaches σ_2. This shows that the precision of the higher frequency band is the limiting factor on the precision of the infinite-frequency ToA.

by σ_2. In PTA data, the smallest ToA uncertainty is often obtained at 1.4 GHz, so observations at lower frequencies should be used to correct for DM variability. In the case of the LOFAR observations presented in this paper, a frequency-integrated ToA uncertainty of $\sim 100\,\mu$s or better would be required to not dominate DM corrections at the $1\,\mu$s-level. This condition is fulfilled for all pulsars in our sample except for PSR J0621+1001, which is a pulsar that is usually timed at an RMS much worse than $1\,\mu$s (see e.g. Desvignes et al. 2016). This shows that approach II should be preferred over approach I, if it is applicable.

To illustrate the superiority of approach II over approach I, we will go through an example of correcting for the dispersive delay in 1.4 GHz observations using LOFAR. We assume $\nu_1 = 1.4\,\mathrm{GHz}$, $\sigma_1 = 1\,\mu$s, $\nu_2 = 150\,\mathrm{MHz}$ and $\sigma_2 = 100\,\mu$s. We note that a ToA precision of $100\,\mu$s is a worst-case scenario. Using approach II, we get $\sigma_{T_\infty} = 1.5\mu$s. For approach I, we assume ten ToAs across a bandwidth of 75 MHz, each with an uncertainty of $\sqrt{10} \cdot 100\,\mu$s and use Equation 10 of Lee et al. (2014) to compute the DM uncertainty. The resulting uncertainty on T_∞ is $3.8\,\mu$s, which is worse by a factor of 2.5.

A major caveat of using LOFAR observations for DM corrections at higher frequencies lies in the spectra of pulsars: pulsars with steep spectra are bright at low frequencies and allow for highly-precise DM corrections, but are fainter at high frequencies, such that the timing precision is so low that DM corrections are less relevant. On the other hand, pulsars with flatter spectra tend to have a high ToA precision at high frequencies, but are very faint at low frequencies due to the steep spectral index of the sky background noise. For example, the pulsar with the best DM precision in our sample is PSR J0034−0534, but its timing RMS at 1.4 GHz is only average (see Verbiest et al. 2016). The well-timed PSR J1713+0747 however is so faint we cannot even detect it in GLOW data and achieve a DM precision an order of magnitude worse than for PSR J0034−0534.

From this follows that approach I using LOFAR data would currently not improve the PTA timing precision for most sources, which could be solved by increasing the timing precision of steep-spectrum sources at 1.4 GHz or improving the DM precision of flat-spectrum sources at low frequencies. The latter could be achieved by greatly increasing the integration time with the LOFAR core or using more sensitive telescopes like the upcoming SKA-LOW. Using a slightly higher frequency might also help if the spectrum of the pulsar is very flat – the optimal frequency for the DM measurement is strongly pulsar dependent. When PTAs manage to increase the timing precision of steep-spectrum sources, they will come to a level where the highly-precise DM time series from our analysis become relevant for DM corrections.

However, approach II should already now improve the timing precision of PTAs for many sources, as it is more precise.

4.5. Data Access

Our ToAs, timing models, templates and DM time series are available online on the Bielefeld pulsar group webpage.[9]

5. Conclusions

We presented low-frequency DM time series for 36 MSPs over up to 7.1 years, obtained from LOFAR observations. Except for the pulsars with very high DM uncertainty (i.e. significantly above $10^{-4}\,\mathrm{cm}^{-3}\mathrm{pc}$), all pulsars show significant variations in DM. 11 pulsars show a clear Solar-wind signal in their DM time series that is usually not to be modelled by a spherically-symmetric electron content with constant amplitude. All of the IISM-related DM variations we presented are fully consistent with a Kolmogorov turbulence spectrum.

These LOFAR observations with a centre frequency around 150 MHz could be used to correct variations of the dispersive delays in higher-frequency observations from PTAs. However, there is the caveat that LOFAR often provides a high DM precision for pulsars that are poorly timed at higher frequencies and vice versa. This issue could be reduced by improved telescopes.

Acknowledgements. This paper is partially based on data obtained with the German stations of the International LOFAR Telescope, constructed by ASTRON (van Haarlem et al. 2013), during station-owners time. In this work we made use of data from the Effelsberg (DE601) LOFAR station funded by the Max-Planck-Gesellschaft; the Unterweilenbach (DE602) LOFAR station funded by the Max-Planck-Institut für Astrophysik, Garching; the Tautenburg (DE603) LOFAR station funded by the State of Thuringia, supported by the European Union (EFRE) and the Federal Ministry of Education and Research (BMBF) Verbundforschung project D-LOFAR I (grant 05A08ST1); the Potsdam (DE604) LOFAR station funded by the Leibniz-Institut für Astrophysik, Potsdam; the Jülich (DE605) LOFAR station supported by the BMBF Verbundforschung project DLOFAR I (grant 05A08LJ1); and the Norderstedt (DE609) LOFAR station funded by the BMBF Verbundforschung project D-LOFAR II (grant 05A11LJ1). The observations of the German LOFAR stations were carried out in stand-alone GLOW mode, which is technically operated and supported by the Max-Planck-Institut für Radioastronomie, the Forschungszentrum Jülich and Bielefeld University. We acknowledge support and operation of the GLOW network, computing and storage facilities by the FZ-Jülich, the MPIfR and Bielefeld University and financial support from BMBF D-LOFAR III (grant 05A14PBA) and D-LOFAR IV (grant 05A17PBA), and by the states of Nordrhein-Westfalia and Hamburg. The GLOW observations were carried out during station-owners time and ILT time allocated under project codes LC0_014, LC1_048, LC2_011, LC3_029, LC4_025, LT5_001, LC9_039 and LT10_014. The observations with the LOFAR core were carried out under ILT time allocation codes LC0_011, LC1_027, LC2_010, LT3_001, LC4_004, LT5_003, LC9_041 and LT10_004.

References

Armstrong, J. W., Rickett, B. J., & Spangler, S. R. 1995, ApJ, 443, 209
Arzoumanian, Z., Baker, P. T., Brazier, A., et al. 2018, ApJ, 859, 47

[9] https://www2.physik.uni-bielefeld.de/radio.html

Arzoumanian, Z., Brazier, A., Burke-Spolaor, S., et al. 2015, ApJ, 813, 65
Bates, S. D., Lorimer, D. R., & Verbiest, J. P. W. 2013, MNRAS, 431, 1352
Burke-Spolaor, S., Taylor, S. R., Charisi, M., et al. 2019, A&A Rev., 27, 5
Cordes, J. M., Shannon, R. M., & Stinebring, D. R. 2016, ApJ, 817, 16
Demorest, P. B., Ferdman, R. D., Gonzalez, M. E., et al. 2013, ApJ, 762, 94
Desvignes, G., Caballero, R. N., Lentati, L., et al. 2016, MNRAS, 458, 3341
Donner, J. Y., Verbiest, J. P. W., Tiburzi, C., et al. 2019, A&A, 624, A22
Hobbs, G. & Dai, S. 2017, National Science Review, 4, 707
Hobbs, G., Lyne, A. G., & Kramer, M. 2010, MNRAS, 402, 1027
Hobbs, G. B., Edwards, R. T., & Manchester, R. N. 2006, MNRAS, 369, 655
Hotan, A. W., Bailes, M., & Ord, S. M. 2005, MNRAS, 362, 1267
Hotan, A. W., van Straten, W., & Manchester, R. N. 2004, PASA, 21, 302
Jammalamadaka, S. R. & SenGupta, A. 2001, Topics in Circular Statistics (New Jersey: World Scientific)
Jones, M. L., McLaughlin, M. A., Lam, M. T., et al. 2017, ApJ, 841, 125
Keith, M. J., Coles, W., Shannon, R. M., et al. 2013, MNRAS, 429, 2161
Künkel, L. 2017, Master's thesis, Bielefeld University, Faculty of Physics
Lazarus, P., Karuppusamy, R., Graikou, E., et al. 2016, MNRAS, 458, 868
Lee, K. J., Bassa, C. G., Janssen, G. H., et al. 2014, MNRAS, 441, 2831
Lorimer, D. R. & Kramer, M. 2005, Handbook of Pulsar Astronomy (Cambridge University Press)
Manchester, R. N., Hobbs, G. B., Teoh, A., & Hobbs, M. 2005, AJ, 129, 1993
Noutsos, A., Sobey, C., Kondratiev, V. I., et al. 2015, A&A, 576, A62
Sanidas, S., Cooper, S., Bassa, C. G., et al. 2019, A&A, 626, A104
Stappers, B. W., Hessels, J. W. T., Alexov, A., et al. 2011, A&A, 530, A80
Taylor, J. H. 1992, Philos. Trans. Roy. Soc. London A, 341, 117
Tiburzi, C. 2018, PASA, 35, e013
Tiburzi, C., Verbiest, J. P. W., Shaifullah, G. M., et al. 2019, MNRAS, 487, 394
van Haarlem, M. P., Wise, M. W., Gunst, A. W., et al. 2013, A&A, 556, A2
van Straten, W. & Bailes, M. 2011, PASA, 28, 1
van Straten, W., Demorest, P., & Oslowski, S. 2012, Astronomical Research and Technology, 9, 237
Verbiest, J. P. W., Bailes, M., Coles, W. A., et al. 2009, MNRAS, 400, 951
Verbiest, J. P. W., Lentati, L., Hobbs, G., et al. 2016, MNRAS, 458, 1267
You, X.-P., Hobbs, G., Coles, W., et al. 2007, MNRAS, 378, 493